Journal of Electronic Imaging

SPIEDigitalLibrary.org/jei

Gradient-based image deconvolution

Heyan Huang
Hang Yang
Siliang Ma

Gradient-based image deconvolution

Heyan Huang
Jilin University
School of Mathematics
Changchun 130012, China
E-mail: huanghy10@mails.jlu.edu.cn

Hang Yang
Changchun Institute of Optics Fine Mechanics and Physics
Chinese Academy of Science
Changchun 130033, China

Siliang Ma
Jilin University
School of Mathematics
Changchun 130012, China

Abstract. *Image restoration and deconvolution from blurry and noisy observation is known to be ill-posed. To stabilize the recovery, total variation (TV) regularization is often utilized for its beneficial edge in preserving the image's property. We take a different approach of TV regularization for image restoration. We first recover horizontal and vertical differences of images individually through some successful deconvolution algorithms. We restore horizontal and vertical difference images separately so that each is more sparse or compressible than the corresponding original image with a TV measure. Then we develop a novel deconvolution method that recovers the horizontal and vertical gradients, respectively, and then estimate the original image from these gradients. Various experiments that compare the effectiveness of the proposed method against the traditional TV methods are presented. Experimental results are provided to show the improved performance of our method for deconvolution problems.*
 [DOI: 10.1117/1.JEI.22.1.013006]

1 Introduction

Image blurring is one of the prime causes of poor quality in digital images. The degradation procedure is often modeled as the result of a convolution with a low-pass filter

$$f(n,m) = \mathcal{H}u(n,m) + \eta(n,m) = (h * u)(n,m) + \eta(n,m), \tag{1}$$

where u and f are the original image and the observed image, respectively. η is the noise produced in the processing of image acquisition, and it is generally assumed to be independent and identically distributed (i.i.d.) zero mean additive white Gaussian noise (AWGN) with variance σ^2, and "*" denoting the convolution operator. In the image deconvolution process, h represents the point-spread function (PSF) of a linear invariant system $\mathcal{H}$. Mathematically, computing u from Eq. (1) can be often modeled as deconvolution process. The difficulty of such a modeling is that the computation of u by direct inversion of h is not reasonable due to noise corruption, thus the problem Eq. (1) is usually ill-posed. Hence, in order to solve this ill-posed problem, one needs to have some prior knowledge of the kind of typical images expected to be restored. This prior information should help to recover the missing information. Usually, it is standard to approach the inverse problem by the regularization method.

In recent years, a number of deconvolution algorithms have been proposed. In these methods, the Wiener filter[1,2] and constrained least squares algorithm[1] can solve this problem in the frequency domain at a fast speed. However, they often obtain a noisy result with ringing effects. A popular regularization is total variation (TV). The TV deconvolution method finds approximate solutions to differential equations in the space of bounded variation (BV) functions. The space of BV functions is a reasonable functional model for images since it contains piecewise smooth functions that allow for discontinuities. The standard total variation (TV) image denoising method estimates the original image by solving the following minimization problem

$$\hat{u} = \underset{u}{\operatorname{argmin}} \|f - u\|^2 + \lambda \mathrm{TV}[u], \tag{2}$$

where $\|\cdot\|$ is the L_2 norm of the function and $\mathrm{TV}[u] = \int_\Omega |\nabla u|$ is the total variation norm of u. The TV functional was first proposed by Rudin, Osher and Fatemi in Ref. 3 in context of image denoising. An adaptive total variation image deconvolution method on the use of majorization-minimization (MM) algorithm was proposed in Ref. 4. This method can achieve good performance even when compared with approaches where the regularization parameter is hand-tuned for optimal performance. It has proved to be particularly relevant in recovering piecewise smooth functions without smoothing sharp discontinuities. Due to its virtue of preserving edges, it is widely used in many applications of

Paper 12124 received Apr. 8, 2012; revised manuscript received Nov. 14, 2012; accepted for publication Dec. 5, 2012; published online Jan. 7, 2013.

0091-3286/2013/$25.00 © 2013 SPIE and IS&T

image processing, such as deconvolution/denoising[5–10] and decomposition.[11–13] A hybrid regularization based on TV and an L_1-norm applied on wavelet coefficients is proposed in Ref. 14 in order to deal with deconvolution in the presence of Gaussian noise. In Ref. 15, Neelamani et al. proposed an efficient, hybrid Fourier-wavelet regularized deconvolution (ForWaRD) algorithm. The ForWaRD method may lead to good results via tandem scalar shrinkages in both the Fourier and wavelet domain. However, in some cases the restored images have slightly low contrast and ripple artifacts. An extension in terms of Shearlet and incomplete measurements, known as ShearDec, ForIcM was proposed in Refs. 16 and 17, respectively. The basic idea for these approaches is that images can be sparsely approximated by properly designed frames, and hence the regularization used for wavelet frame based models is the l_1-norm of frame coefficients.

The images of interest tend to enjoy the property of being sparse or compressible in some transform domain (e.g., wavelet,[15] gradient,[18] Fourier,[15] etc). Images are inherently sparse in the pixel or gradient domain. For instance, if the image is piecewise-constant, then a gradient representation would only contain non-zero values near boundary positions, we say that it is sparse with respect to the total variation (TV) measure. Most TV-based image deconvolution approaches minimize the TV semi-norm, which enforces the necessary TV sparsity of the solution (see Refs. 5 to 10, and others). The fast total variation deconvolution (FTVd)[19] method is a state-of-the-art algorithm for TV-based image deconvolution and it solves TV minimization by augmented Lagrangian and alternating direction algorithms. The main idea of the FTVd method is to reformulate a TV problem as a linear equality constrained problem where the objective function is separable, and then minimize its augmented Lagrangian function using Gauss-Seidel updates of both primal and dual variables. The FTVd method can generally achieve better quality faster than several iterative methods for TV image restoration.[20–22]

The previous TV-based deconvolution method does not take advantage of the additional sparsity, which is utilizing the two horizontal and vertical directional derivatives of the image. The total variation-based image denoising/deblurring model has been generalized and extended in numerous ways, improving its performance in different contexts.[23] Sparse-gradient images are more sparse under differences in a single direction than in the TV sense. By exploiting this, we present a different approach to the problem of recovering a sparse-gradient image from the blurred image in this paper. By using the fact that the Fourier transform of the gradients of an image are precisely equal to a diagonal transformation of the Fourier transform of the original image, we utilize TV methods to directly recover the horizontal and vertical differences of our desired image. Then, we recover the original image from our edge estimates by solving a simple penalized least-square (LS) optimization problem.

The rest of the paper is organized as follows: In Sec. 2 we briefly describe our problem formulation and notations used in our paper. We motivate and present our deconvolution framework and an efficient algorithm that implements the proposed approach is developed in Sec. 3. Section 4 addresses the numerical implementation for deconvoluting images problem efficiently and presents several experimental results. We finally draw a conclusion in Sec. 5.

2 Notation and Problem Formulation

In this paper, we will utilize the following notational conventions when dealing with images. Let $u \in R^{N\times M}$ denote an image. Any particular pixel of u will be written as $u_{n,m}$ or $u(n,m)$ depending on whichever is more convenient in any given setting.

The discrete directional derivatives on x and y are defined pixel-wise as

$$(u_x)_{n,m} = u_{n,m} - u_{n-1,m} \tag{3}$$

$$(u_y)_{n,m} = u_{n,m} - u_{n,m-1}. \tag{4}$$

Based on these, the discrete gradient operator ∇ where $\nabla u \in R^{N\times M\times 2}$ is defined as

$$(\nabla u)_{n,m} = [(u_x)_{n,m}, (u_y)_{n,m}]. \tag{5}$$

From these operators, one can define the discrete TV operator on u as

$$[\mathrm{TV}(u)]_{n,m} = \sqrt{|(u_x)_{n,m}|^2 + |(u_y)_{n,m}|^2}, \tag{6}$$

from which one can also define the TV seminorm of u as

$$\|u\|_{\mathrm{TV}} = \|\mathrm{TV}[u]\|_1, \tag{7}$$

where $\|\cdot\|_1$ is the l_1 norm defined as

$$\|u\|_1 = \sum_{n=1}^{N}\sum_{m=1}^{N} |u_{n,m}|. \tag{8}$$

To that end, let $\mathcal{F}$ denote the 2-D DFT of u and $\mathcal{F}^{-1}$ its inverse.

3 Description of the Proposed Scheme

In this paper, we use the TV measure in horizontal and vertical differences images, respectively, and not in an observed image, such as traditional TV-based deconvolution methods. Figure 1 shows the flowchart of our method. It is possible to embed any of the various TV-based deconvolution algorithms (such as alternating minimization, iterative thresholding algorithms, nonconvex algorithms and convex optimization algorithms) for solving the traditional TV model. We show that, instead of restoring an image by TV minimization, one can restore the image by separately restoring the horizontal and vertical differences, and then integrate two parts to obtain the final estimate image. Traditional image deconvolution methods of TV-based regularization utilize the sparsity of TV measure, which can be expressed approximately as l_1 norm. Figure 2 presents an important comparison in the sparsity of $[u_x]$, $[u_y]$, and u under the TV measure, where u_x and u_y are the vertical and horizontal difference images of u, respectively. The plots of the sorted absolute values of the coefficients of gradients TV $[u_x]$, TV $[u_y]$, and TV $[u]$ for the Barbara images (see Fig. 2) indicate that TV $[u_x]$, TV $[u_y]$ decay much faster than the TV measure. In fact, it is easy to see from Fig. 2 that the coefficients of TV

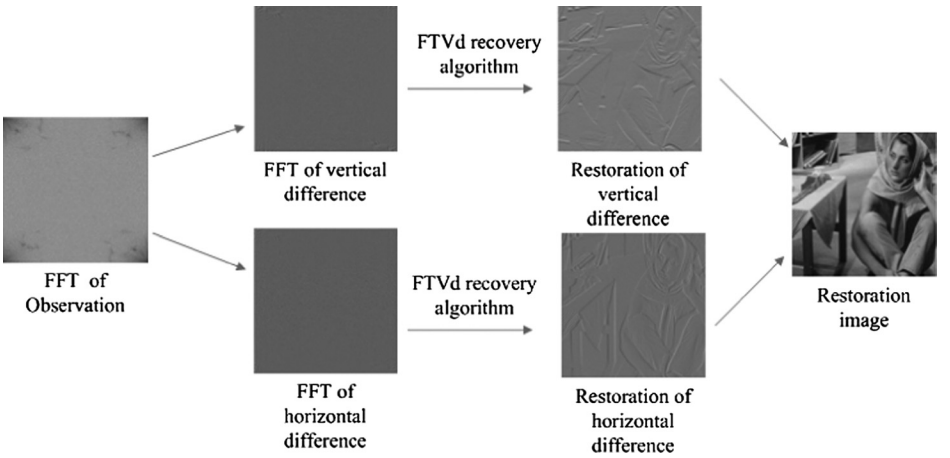

Fig. 1 Flowchart of our method.

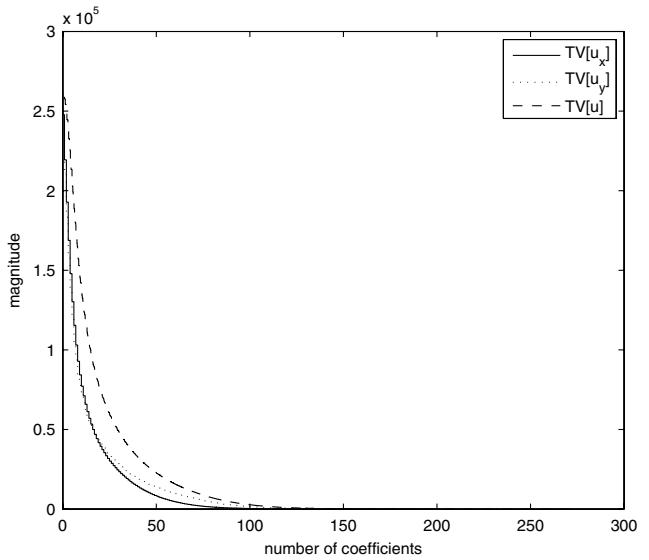

Fig. 2 Magnitude of TV $[u]$, TV $[u_x]$, TV $[u_y]$ coefficients in decreasing order for Barbara image.

$[u_x]$ and TV $[u_y]$ decay faster than the coefficients of TV $[u]$. This means that our method can take advantage of this and can be able to restore a more sparse image under the difference measure than the traditional TV-based method.

Our algorithm consists of three main steps.

1. The discrete Fourier transform is first utilized on original blur measurements, and obtains the corresponding vertical and horizontal differences in the Fourier space.
2. It then utilizes some algorithms from the suite of image recovery routines (e.g., FTVd, iterative thresholding algorithm, alternating direction method of multipliers (ADMM), etc.) to recover the difference images.
3. Finally, it recovers the original image from the estimates of its differences and observed image by minimizing the least-square (LS) error function.

In order to get horizonal and vertical differences images, we use the fact that the Fourier transform of the gradients of an image are precisely equal to a diagonal transformation of the Fourier transform of the original image. Here, we give a simple deduction of vertical difference image u_x, and horizontal difference image u_y is obtained likewise. The discrete Fourier transform of image u could be written as

$$\mathcal{F}(u)_{k_1,k_2} = \sum_{n,m} u_{n,m}\, e^{-i2nk_1\pi/N} e^{-i2mk_2\pi/M}, \tag{9}$$

and DFT of vertical difference image could be written as

$$\begin{aligned}\mathcal{F}(u_x)_{k_1,k_2} &= \sum_{n,m} (u_x)_{n,m}\, e^{-i2nk_1\pi/N} e^{-i2mk_2\pi/M} \\ &= \sum_{n,m} (u_{n,m} - u_{n-1,m})\, e^{-i2nk_1\pi/N} e^{-i2mk_2\pi/M} \\ &= (1 - e^{-i2k_1\pi/N}) \sum_{n,m} u_{n,m}\, e^{-i2nk_1\pi/N} e^{-i2mk_2\pi/M} \\ &= (1 - e^{-i2k_1\pi/N}) \mathcal{F}(u)_{k_1,k_2}.\end{aligned}$$

Given blurred observations f, we first obtain Fourier observations $\mathcal{F}f$ through fast Fourier transform, then we get the Fourier observations of f_x and f_y based on the above fact through the following equation

$$\begin{aligned}(\mathcal{F}f_x)_{\mathbf{k}} &= (1 - e^{-2\pi i k_1/N})(\mathcal{F}f)_{\mathbf{k}} \\ (\mathcal{F}f_y)_{\mathbf{k}} &= (1 - e^{-2\pi i k_2/M})(\mathcal{F}f)_{\mathbf{k}},\end{aligned}$$

where $\mathbf{k} = (k_1, k_2)$, $1 \le k_1 \le N$, $1 \le k_2 \le M$. After this is done, we get the horizonal and vertical differences images in Fourier domain, and thus we can obtain edge images of blurry observations. Many image deconvolution algorithms can be used to recover u_x and u_y from their respective Fourier observations. For instance, we assume that the observations are of the following form:

$$f_x = h * u_x + \eta_x \quad f_y = h * u_y + \eta_y,$$

where $(\eta_x)_{\mathbf{k}} = \mathcal{F}^{-1}[(1 - e^{-2\pi i k_1/N})(\mathcal{F}\eta)_{\mathbf{k}}]$ and $(\eta_y)_{\mathbf{k}} = \mathcal{F}^{-1}[(1 - e^{-2\pi i k_2/M})(\mathcal{F}\eta)_{\mathbf{k}}]$. This assumption is based on the properties of convolution:

$$\frac{\partial(h*u)}{\partial x} = h * \frac{\partial u}{\partial x} \quad \frac{\partial(h*u)}{\partial y} = h * \frac{\partial u}{\partial y}.$$

After that is done, we use the following unconstrained forms to solve u_x and u_y from the previous two equations

$$\hat{u}_x = \underset{u_x}{\operatorname{argmin}} \|u_x\|_{\mathrm{TV}} + \frac{\lambda_1}{2}\|h * u_x - f_x\|_2^2$$

$$\hat{u}_y = \underset{u_y}{\operatorname{argmin}} \|u_y\|_{\mathrm{TV}} + \frac{\lambda_2}{2}\|h * u_y - f_y\|_2^2.$$

Then gradients can be estimated by the FTVd method to solve the previous two optimization problems. After obtaining estimates $\hat{u}_x$ and $\hat{u}_y$ of u_x and u_y, respectively, some kind of integration must be performed to recover estimates $\hat{u}$ of u. In order to obtain u from f, $\hat{u}_x$ and $\hat{u}_y$, we adopt the lease-square method that was proposed in Ref. 18, and solve the following optimization problem:

$$\hat{u} = \underset{u}{\operatorname{argmin}} \|u_x - \hat{u}_x\|^2 + \|u_y - \hat{u}_y\|^2 + \beta\|u\|_{\mathrm{TV}} + \lambda\|u * h - f\|^2, \tag{10}$$

where β and λ are penalty parameters that determine the degrees to which the TV minimization and fidelity constraints are enforced. Following the previous definition of TV, solving optimization problem Eq. (10) can be time-consuming and difficult. Following Ref. 18, one can replace the intrinsic l_1 norm associated with the TV norm in (2.5) with an l_2 norm. This changes Eq. (10) into the following least square (LS) optimization problem:

$$\hat{u} = \underset{u}{\operatorname{argmin}} \|u_x - \hat{u}_x\|^2 + \|u_y - \hat{u}_y\|^2 + \beta(\|u_x\|^2 + \|u_y\|^2) + \lambda\|u * h - f\|^2. \tag{11}$$

Due to the existence of the convolution operator, we use fast Fourier transform (FFT) for speed up. We rewrite Eq. (11) as the following equivalent problem in the Fourier domain:

$$\hat{U} = \underset{U}{\operatorname{argmin}} \|A_1 U - \hat{U}_x\|^2 + \|A_2 U - \hat{U}_y\|^2 + \beta(\|A_1 U\|^2 + \|A_2 U\|^2) + \lambda\|UH - F\|^2. \tag{12}$$

where $A_1 = 1 - e^{-i2k_1\pi/N}$, $A_2 = 1 - e^{-i2k_2\pi/M}$, and $\hat{U}$, $\hat{U}_x$, $\hat{U}_y$, U, H, F are the FFT of $\hat{u}$, $\hat{u}_x$, $\hat{u}_y$, u, h, f, respectively. Then, we can write the solution of (3.4) directly:

$$\hat{U} = \frac{\bar{A}_1\hat{U}_x + \bar{A}_2\hat{U}_y + \lambda\bar{H}F}{(1+\beta)(\bar{A}_1A_1 + \bar{A}_2A_2) + \lambda\bar{H}H}, \tag{13}$$

where $\bar{A}_1$, $\bar{A}_2$ and $\bar{H}$ are the complex conjugate of A_1, A_2 and H, respectively. The addition, multiplication, and division are all component-wise operators. Compared to minimizing Eq. (10) directly in the image space, which involves very-large-matrix inversion, computation in the Fourier domain is much faster due to the simple component-wise division.

4 Experimental Results

In this section, we present results of our proposed method and compare them with some of the deconvolution methods, such as traditional TV-based image restoration methods solved by FTVd,[19] ForWaRD,[15] TVMM.[4] In order to validate our approach with respect to the tested methods, we use the statistical measure improved signal-to-noise ratio (ISNR), SNR and the structural similarity index (SSIM), which are often used in image restoration to measure the performance. These definitions are:

$$\mathrm{ISNR} = 10\log_{10}\left(\frac{\|u-f\|_2}{\|u-\hat{u}\|_2}\right)$$

$$\mathrm{SNR} = 10\log_{10}\left(\frac{\|u\|_2}{\|u-\hat{u}\|_2}\right)$$

$$\mathrm{SSIM} = \frac{(2\mu_u\mu_{\hat{u}} + C_1)(2\sigma_{u\hat{u}} + C_1)}{(\mu_x^2 + \mu_y^2 + C_1)(\sigma_u^2 + \sigma_{\hat{u}}^2 + C_2)},$$

where f, u, and $\hat{u}$ are the observed image, original image and recovered image, μ_u and $\mu_{\hat{u}}$ are (respectively) the means of u and $\hat{u}$, σ_u and $\sigma_{\hat{u}}$ are (respectively) the standard deviations of u and $\hat{u}$, and $\sigma_{u\hat{u}}$ is the cross correlation of u and $\hat{u}$ after removing their means. The items C_1, C_2 are small positive constants that stabilize each term. In our experiments, we set $C_1 = 0.01$, $C_2 = 0.03$ for the experiments.

We consider nine benchmark deblurring problems. In these experiments, original images (Fig. 3) are Barbara (experiments 1, 2 and 3), Lena (experiments 4, 5, 6 and 7) and Tower (experiments 8 and 9). Table 1 summarizes the

(a) Barbara image (b) Lena image (c) Tower image

Fig. 3 Images used in this paper for different experiments.

Table 1 Images, Blur PSF and noise variance used in each experiment.

	Blur	σ^2
Exp.1	$v(i,j) = 1/(+i^2+j^2)$, $i, j = -1, \cdots, 7$ (Barbara)	2
Exp.2	$v(i,j) = 1/(+i^2+j^2)$, $i, j = -1, \cdots, 7$ (Barbara)	8
Exp.3	v is a Gaussian PSF with standard deviation 1.6 (Barbara)	4
Exp.4	$v = [14641]^T[14641]/256$ (Lena)	49
Exp.5	$v(i,j) = 1/(+i^2+j^2)$, $i, j = -1, \cdots, 7$ (Lena)	2
Exp.6	$v(i,j) = 1/(+i^2+j^2)$, $i, j = -1, \cdots, 7$ (Lena)	8
Exp.7	v is a Gaussian PSF with standard deviation 1.6 (Lena)	4
Exp.8	$v(i,j) = 1/(+i^2+j^2)$, $i, j = -1, \cdots, 7$ (Tower)	2
Exp.9	$v(i,j) = 1/(+i^2+j^2)$, $i, j = -1, \cdots, 7$ (Tower)	8

Table 2 ISNR for different experiments.

Exp.	Our method	ForWaRD	FTVd	TVMM
Exp.1	**4.43**	3.69	3.49	3.10
Exp.2	**2.34**	1.87	1.67	1.33
Exp.3	**1.01**	0.98	0.90	0.75
Exp.4	**3.80**	2.93	3.60	3.52
Exp.5	**7.11**	6.05	6.38	6.36
Exp.6	**5.48**	4.90	5.12	4.98
Exp.7	**3.73**	3.50	3.44	3.61
Exp.8	**7.49**	7.40	7.06	6.85
Exp.9	**5.31**	5.03	4.90	4.88

Table 3 SNR for different experiments.

Exp.	Our method	ForWaRD	FTVd	TVMM
Exp.1	**21.82**	20.85	20.92	20.49
Exp.2	**19.70**	18.98	19.03	18.69
Exp.3	**18.85**	18.64	18.64	18.59
Exp.4	**26.89**	26.02	26.74	26.62
Exp.5	**28.71**	27.66	28.01	27.96
Exp.6	**26.85**	26.29	26.50	26.35
Exp.7	**27.24**	26.96	26.94	27.11
Exp.8	**24.98**	4.71	24.53	24.34
Exp.9	**22.73**	22.32	22.32	22.30

Table 4 SSIM for different experiments.

Exp.	Our method	ForWaRD	FTVd	TVMM
Exp.1	**0.9344**	0.9216	0.9225	0.8351
Exp.2	**0.8805**	0.8702	0.8655	0.7666
Exp.3	**0.8720**	0.8714	0.8685	0.7961
Exp4.	**0.9536**	0.9489	0.9526	0.8059
Exp.5	**0.9723**	0.9622	0.9693	0.8796
Exp.6	**0.9553**	0.9477	0.9517	0.8250
Exp.7	**0.9687**	0.9611	0.9629	0.8807
Exp.8	**0.9647**	0.9569	0.9539	0.7952
Exp.9	**0.9354**	0.9309	0.9125	0.7614

different degradation models used, which are defined by the blur type, the variance of the AWGN for each of the experiments. We mark the highest experiment values in bold. Through the marking values we can see the effectiveness of the algorithm more clearly.

Sparse-gradient images are more sparse under differences in a single direction than in the TV sense. By exploiting it, we develop a novel deconvolution method that recovers the horizontal and vertical gradients, respectively, and then estimate the original image from these gradients. In order to validate the effectiveness of our algorithm, we have compared the ISNR and SNR, and SSIM results given by our approach and the other published deconvolution methods, respectively, in Tables 2–4. These present a comparison of the ISNR, SNR, and SSIM for Barbara, Lena, and Tower images for a few deconvolution methods (FTVd,[19] ForWaRD,[15] TVMM[4]), respectively. From these numerical performances, one can see that our method obtains good results in most cases in terms of ISNR, SNR, and SSIM. The results of ForWaRD[15] are obtained with the Matlab codes[24] made available by its authors, for which we used automatically estimated regularization parameters. The results for TVMM[4] are obtained by the software available online and the results of FTVd are obtained with the Matlab codes[25] made available by its authors. In order to fairly compare the results, we have tuned the parameters to achieve the best quality of the restoration images for our method. In most of the experiments, the proposed method outperforms the few deconvolution methods in terms of ISNR, SNR, and SSIM. We notice that our method leads to competitive restoration results for various level of

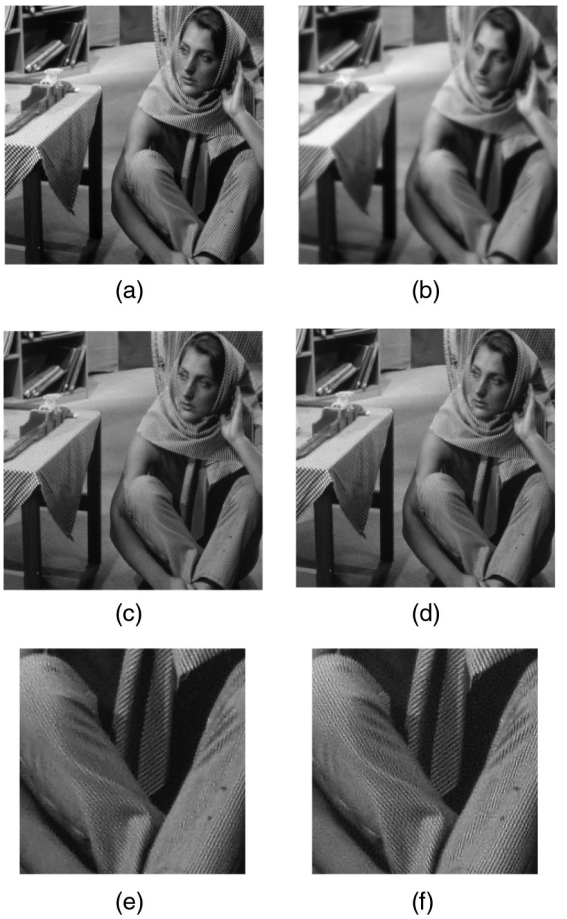

Fig. 4 The result of the first experiment with Barbara image. From left to right, from top to bottom. (a) Original image. (b) Noisy blurred image. (c) FTVd estimate, ISNR = 3.49, SNR = 20.92, SSIM = 0.9225. (d) Our algorithm estimate, ISNR = 4.43, SNR = 21.82, SSIM = 0.9344. (e) Fragments of the FTVd result. (f) Fragments of the result by our method.

blur and noise degradations in the experiments compared with a few deconvolution methods.

In Fig. 4, we show the restored and zoomed images of experiment 1 for "Barbara" image, where a comparison with the FTVd deblurring is made. One can see that fine details are well preserved and there are few artifacts in the deblurred image. The zoomed image of the FTVd algorithm is shown in Fig. 4(e). By carefully examination, some image textures on the trousers are lost, and it has slightly lower contrast on the trousers. Figure 4(f) shows the restoration result of our proposed method, showing how much more visually pleasant and brighter it is than Fig. 4(e) and how it obtains more details. In Fig. 4, fine details are well preserved and there are few artifacts in the deblurred images utilizing our proposed method.

In addition, the visual quality of other restored "Barbara" images can be evaluated in Fig. 5 that we show the result of experiment 2 and experiment 3, respectively. Here the image textures on the trousers and headkerchief are well preserved in the deblurred images. From Tables 2–4, we can see that our results also perform well in terms of ISNR, SNR, and SSIM.

We have also done the experiments on the "Lena" image. The comparison between FTVd method and our proposed method, and zommed restoration results of the experiment 7

Fig. 5 Deblurring results of our method for Barbara. (a) Noisy blurred image (Exp.2). (b) Output: ISNR = 2.34, SNR = 19.70, SSIM = 0.8805. (c) Noisy blurred image (Exp.3). (d) Output: ISNR = 1.01, SNR = 18.85, SSIM = 0.8720.

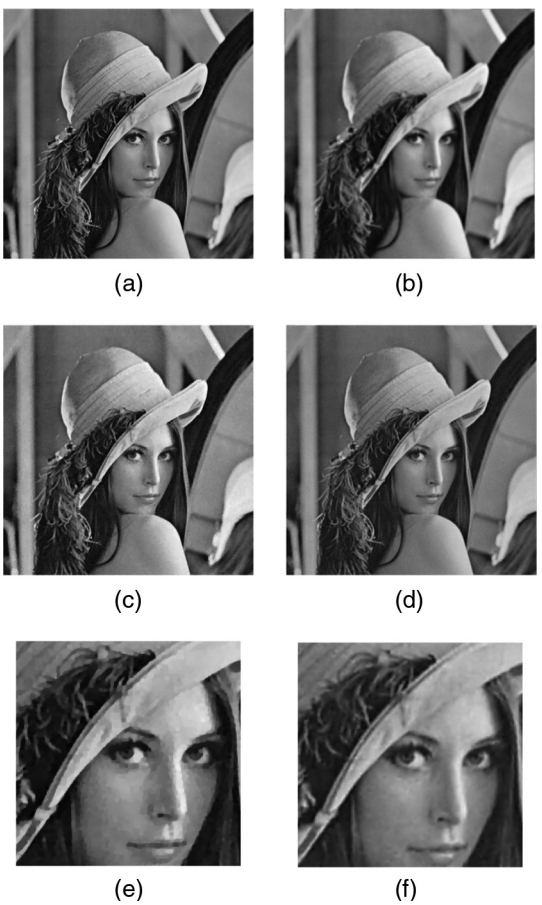

Fig. 6 The result of the seventh experiment with Lena image. From left to right, from top to bottom. (a) Original image. (b) Noisy blurred image. (c) FTVd estimate, ISNR = 3.44, SNR = 26.94, SSIM = 0.9629. (d) Our algorithm estimate, ISNR = 3.73, SNR = 27.24, SSIM = 0.9687. (e) Fragments of the FTVd result. (f) Fragments of the result by our method.

Fig. 7 Deblurring results of our method for Lena. (a) Noisy blurred image (Exp.4). (b) Output: ISNR = 3.80, SNR = 26.89, SSIM = 0.9536. (c) Noisy blurred image (Exp.5). (d) Output: ISNR = 7.11, SNR = 28.71, SSIM = 0.9723. (e) Noisy blurred image (Exp.6). (f) Output: ISNR = 5.48, SNR = 26.85, SSIM = 0.9553.

are shown in Fig. 6. From Fig. 6(e), we can see that some textures, such as eyelashes are lost and the bongrace (hat) produces the ring effort. The restoration result of our proposed method is shown in Fig. 6(f). One can see that our method achieves better visual result and obtain more textures. The quality of other experiments of the "Lena" image can be seen in Fig. 7. Analyzing these figures, we can see that the proposed algorithm is able to suppress the ringing artifacts better than other compared methods and provides sharper image edges. Figure 8 shows the observations and the corresponding restored images for "Tower" image. Both the objective and subjective quality of our estimates are high.

5 Conclusions

As sparse-gradient images are more sparse under differences in a single direction than in the TV sense, it follows that increased accuracy will be possible when linear differences of such images are recovered utilizing FTVd algorithms. We first recover the horizontal and vertical difference images, respectively. From these linear differences, one can employ the integration method to recover the original image. Through extensive experimentation, we have shown that the proposed algorithm in this paper, which combines edge estimation via FTVd with the integration method, offers

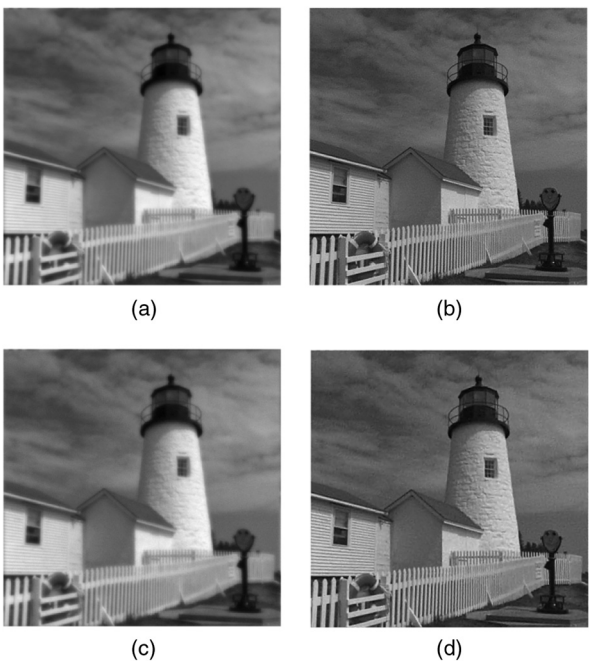

Fig. 8 Deblurring results of the proposed method for Tower. (a) Noisy blurred image (Exp.8). (b) Output: ISNR = 7.49, SNR = 24.98, SSIM = 0.9647. (c) Noisy blurred image (Exp.9). (d) Output: ISNR = 5.31, SNR = 22.73, SSIM = 0.9354.

significant improvement in restoration quality and robustness over leading TV minimizers in various deblurring scenarios.

References

1. A. K. Katsaggelos, *Digital Image Restoration*, Springer-Verlag, New York (1991).
2. P. C. Hansen, *Rank-Deficient and Discrete Ill-Posed Problems: Numerical Aspects of Linear Inversion* SIAM, Philadelphia (1998).
3. L. I. Rudin, S. Osher, and E. Fatemi, "Nonlinear total variation based noise removal algorithms," *Phys. Nonlinear Phenom.* **60**(1–4), 259–268 (1992).
4. J. Oliveira, J. M. Bioucas-Dias, and M. A. Figueiredo, "Adaptive total variation image deblurring: a majorization-minimization approach," *Signal Process.* **89**(9), 1683–1693 (2009).
5. A. Chambolle and P.-L. Lions, "Image recovery via total variation minimization and related problems," *Numer. Math.* **76**(2), 167–188 (1997).
6. T. F. Chan and C. K. Wong, "Total variation blind deconvolution," *IEEE Trans. Image Process.* **7**(3), 370–375 (1998).
7. T. Chan, A. Marquina, and P. Mulet, "High-order total variation-based image restoration," *SIAM J. Sci. Comput.* **22**(2), 503–516 (2000).
8. F. Malgouyres, "Minimizing the total variation under a general convex constraint for image restoration," *IEEE Trans. Image Process.* **11**(12), 1450–1456 (2002).
9. L. He, A. Marquina, and S. Osher, "Blind deconvolution using TV regularization and Bregman iteration," *Int. J. Imag. Syst. Technol.* **15**(1), 74–83 (2005).
10. A. Marquina, "Nonlinear inverse scale space methods for total variation blind deconvolution," *SIAM J. Imag. Sci.* **2**(1), 64–83 (2009).
11. L. A. Vese and S. Osher, "Modeling textures with total variation minimization and oscillating patterns in image processing," *J. Sci. Comput.* **19**(1–3), 553–572 (2003).
12. L. A. Vese and S. Osher, "Image denoising and decomposition with total variation minimization and oscillatory functions," *J. Math. Imag.* **20**(1–2), 7–18 (2004).
13. W. Yin, D. Goldfarb, and S. Osher, "Total variation based image cartoon-texture decomposition," Columbia University CORC Report TR-2005-01, UCLA CAM Report 05-27 (2005).
14. P. L. Combettes and J.-C. Pesquet, "A proximal decomposition method for solving convex variational inverse problems," *Inverse Probl.* **24**(6), 2450–2461 (2008).
15. R. Neelamani, H. Choi, and R. G. Baraniuk, "Forward: Fourier-wavelet regularized deconvolution for ill-conditioned systems," *IEEE Trans. Signal Process.* **52**(2), 418–433 (2004).

16. V. M. Patel, G. R. Easley, and D. M. Healy, "Shearlet-based deconvolution," *IEEE Trans. Image Process.* **18**(12), 2673–2685 (2009).
17. H. Yang and Z. B. Zhang, "Image deblurring based on ForIcM: Fourier shrinkage and incomplete measurements," *Imag. Sci. J.* **60**(6), 344–351 (2012).
18. V. M. Patel, R. Maleh, A. C. Gilbert, and R. Chellappa, "Gradient-based image recovery methods from incomplete Fourier measurements," *IEEE Trans. Image Process.* **21**(1), 94–105 (2012).
19. J. Yang, W. Yin, Y. Zhang, and Y. Wang, "A fast algorithm for edge-preserving variational multichannel image restoration," *SIAM J. Imag. Sci.* **2**(2), 569–592 (2009).
20. A. Beck and M. Teboulle, "A fast iterative shrinkage-thresholding algorithm for linear inverse problems," *SIAM J. Imag. Sci.* **2**(1), 183–202 (2009).
21. J. Bioucas-Dias and M. Figueiredo, "A new TwIST: two-step iterative shrinkage/thresholding algorithms for image restoration," *IEEE Trans. Image Process.* **16**(12), 2992–3004 (2007).
22. O. V. Michailovich, "An iterative shrinkage approach to total-variation image restoration," *IEEE Trans. Image Process.* **20**(5), 1281–1299 (2011).
23. G. Boracchi and A. Foi, "Modeling the performance of image restoration from motion blur," *IEEE Trans. Image Process.* **21**(8), 3502–3517 (2012).
24. "Forward: Fourier-wavelet regularized deconvolution for ill-conditioned systems," Matlab Codes Version 2.0, http://www.dsp.rice.edu/software/ward.shtml.
25. "A fast algorithm for edge preserving variational multichannel image restoration," FTVd: A MATLAB code for total variation image deblurring, Version 4.1, last update on June, 2010, http://www.caam.rice.edu/optimization/L1/ftvd/.

Heyan Huang is a PhD student at the School of Mathematics, Jilin University. Her present research interests include image processing and pattern recognition.

Hang Yang is a post-PhD at Changchun Institute of Optics, Fine Mechanics and Physics, Chinese Academy of Science. His present research interests include image processing and pattern recognition.

Siliang Ma is a professor at the School of Mathematics, Jilin University. His present research interests include image processing and pattern recognition.